

850nm high pass filter. In addition two single color pyrometer measured the surface temperature at the middle of the plate near the plate edge where the heat flux has a maximum. The temperature of the graphite 140° roof limiter was measured also by two thermocouples immersed through holes into the limiter body. The 2D distribution of the $H_{\beta}(486.1\text{nm})$ line intensity was measured with an intensified CCD camera viewing tangentially to the limiter and equipped with optical interference filter. The main plasma parameters of the TEXTOR discharges were: $I_p = 355 \text{ kA}$, $B_T = 2.25 \text{ T}$, $\bar{n}_e = 4 \cdot 10^{19} \text{ m}^{-3}$, $a = 47.2 \text{ cm}$, $Z_{eff} \sim 1.4$, $P_{NBI} = 1.2 \text{ MW}$ for 5 s, $P_{tot} = 1.4 \text{ MW}$, radiation level $\gamma \approx 0.45$.

Experimental results

The tungsten melting was intended by purpose and occurred only during two discharges with highest heat flux densities to the tungsten plate. The limiter was positioned at plasma radii $r = 45.8 \text{ cm}$ and 46.0 cm during these plasma discharges and a toroidal magnetic field was ramped down from 2 T to 1.1 T over 2.17 s. The increase of the limiter temperature measured by thermocouple was 65°C for a heat pulse duration of 1.7 s that corresponds to a peak heat flux density of about 17 MW/cm^2 at the plate.

For normal discharges with a constant toroidal magnetic field, the heat flux density was $5.5\text{-}6 \text{ MW/cm}^2$ at this limiter position and the surface temperature of the plate was below the melting point of tungsten. The surface temperature distribution on the plate at maximal temperature is shown in fig.1.

The tungsten was molten poloidally along the plate edge at the region of the maximum heat flux as can be seen in fig.2. The liquid tungsten moved perpendicular to the magnetic field lines along the plate surface. The motion of liquid tungsten produced a deep furrow along the plate surface. A large blob of liquid tungsten

was collected at the plate edge, from which then two jets of molten material moved up towards the scrape-off layer plasma along the edge of the graphite roof limiter.

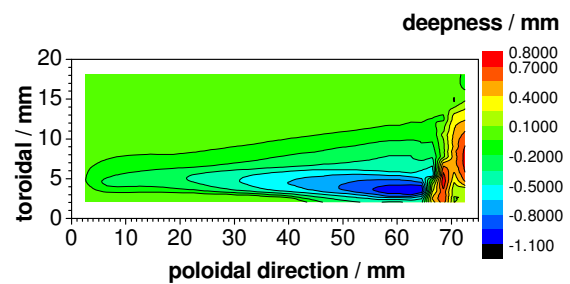


Fig.3 The surface profile in the molten zone.

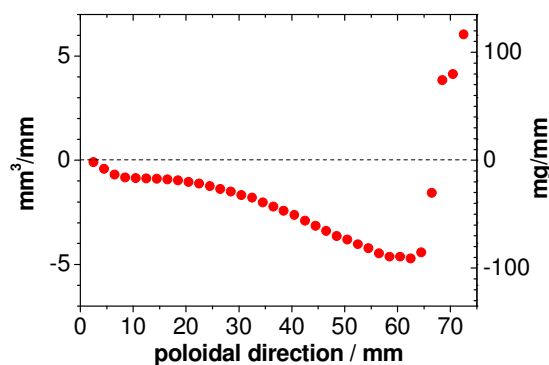


Fig.4 Toroidally integrated tungsten loss

The width of the jets is about 3 mm. The velocity of the liquid jets was estimated to be about 1.5 m/s and is nearly constant within the first 2 cm of motion. The jet propagates over a

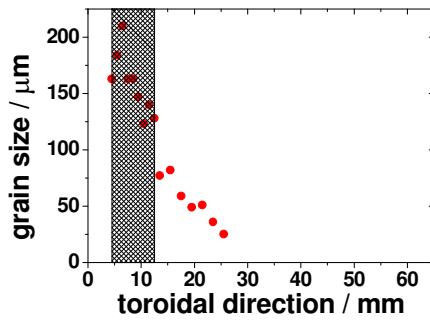


Fig.5 Dependence grain size on the position.

distance of about 5 cm. The melt layer erosion was monitored afterwards by a large scale surface profilometer. The maximal thickness of the melt erosion was 1 mm shown in fig.2. The material loss integrated over the toroidal direction is shown in fig.3. The total material loss integrated over 1 s during the existence of the liquid tungsten was about of 2.85 g. *Ex-situ* surface characterization of the tungsten plate has been performed with a number of techniques. Strong tungsten re-crystallization is found within about 3 cm from the hottest plate side as one can see in fig.5 where the mean size of the grain is shown versus the toroidal direction for middle part of the plate. The marked area indicates the molten zone. Holes with grain shapes are observed on the edges of the erosion zone as shown in fig.6. The re-crystallization of molten material has lead to the formation of larger grains and distinct grain boundaries. No indications of blistering effects are found on the plate, neither in nor outside the melt-layer zone. An island-type inclusions of carbon particles are detected in the eroded region. Small dust-like spherical granules of tungsten are observed. The surface of the graphite limiter behind the hottest part of the plate has a clear visible tungsten coating.

Discussion

The liquid tungsten moved perpendicular to the magnetic field that indicates the electromagnetic nature of the driving force, i.e. the presence of $\mathbf{j} \times \mathbf{B}$ force. The motion continues even in the deep scrape-off layer region where the plasma density decreases. The observed motion of the liquid tungsten is interpreted as due to forces induced by the thermo-electron emission from the hot tungsten plate. The condition for the vertical movement of the liquid tungsten across magnetic field along the electro-conducting wall is $j(T_s) \cdot B > \rho g$, where $j(T) = AT^2 \exp(-e\phi/kT)$ – thermionic current (for tungsten $A = 0.72 \cdot 10^6 \text{ A/m}^2 \text{ K}^2$ and $\phi = 4.54 \text{ eV}$), $\rho = 19.3 \cdot 10^3 \text{ kg/m}^3$ – tungsten density and $g = 9.81 \text{ m/s}^2$. This condition is fulfilled if $T_s > 2990 \text{ K}$ for $B = 1.2 \text{ T}$. One could argue that the estimation of a space-charge limit for the current as given in [2] shows that the thermo-emission current is limited to values of

Fig.6 SEM picture of the edge of the melt erosion region.

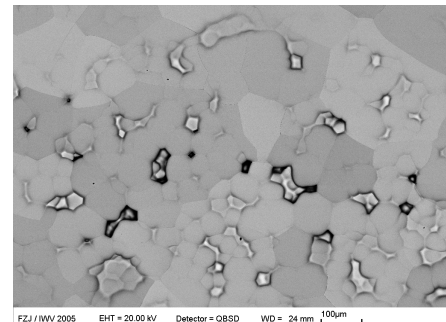


Fig.6 SEM picture of the edge of the melt erosion region.

about $1.4 \cdot 10^6 \text{ A/m}^2$ that is much higher than ion saturation current of about $8.5 \cdot 10^4 \text{ A/m}^2$ for surface temperatures above 3400 K and for parameter of the experiment ($n_e \sim 9 \cdot 10^{18} \text{ m}^{-3}$ and $T_e \sim 35 \text{ eV}$). The critical temperature is below the melting point of tungsten. Therefore, the liquid tungsten can move up on the vertical wall immediately after melting. The maximum stationary melt layer velocity v roughly estimated from $j/\sigma = v \cdot B$ is about of 1.7m/s, where $\sigma \approx 6.9 \cdot 10^5 \text{ } \Omega^{-1} \cdot \text{m}^{-1}$ - the conductivity of liquid tungsten and $j = 1.4 \cdot 10^6 \text{ A/m}^2$ - charge limited current. This value is in a good agreement with the observed velocity of the liquid tungsten jet. The grain size has a maximum size in the melt zone due to the higher temperature and thicker melt layer at this position. The melt erosion increases poloidally in the direction of melt layer motion, as seen in fig.4. The plate shows a slight deformation after the experiments. The right corner of the plate where the liquid material formed a large blob moved up about of 100 μm from its original profile. This deviation value can not be only responsible for observed the melt erosion inhomogeneity, which is rather due to the heat transfer by the movement of the liquid tungsten poloidally across the surface. However, the plasma heat flux distribution may also change due to thermo-electron current, as observed in [3]. The holes shown on fig.6 may be formed, because the temperature in this region is close to the melting point and only grains with reduced thermal contact were molten and removed by electromagnetic forces. The observed small dust-like spherical granules can be a result on such erosion. This indicates a possible formation of tungsten dust from the molten mass in a magnetic controlled fusion device.

Conclusions

Tungsten molten by plasma impact shows a rapid movement of the liquid perpendicular to magnetic field lines. The driving force of this is the $j \times B$ force with the current given by thermo emission of electrons from the hot tungsten surface. In a single shot, 2.85 g of tungsten molten and moved poloidally, forming a deep erosion channel, whose deepness increased poloidally up to a maximum value of about 1 mm. Thermoelectric forces moved the molten droplets upwards against gravity. Large tungsten re-crystallization and carbon inclusions were observed and in addition small holes have been formed. The results show that melting can lead to a large material redistribution without ejection of molten material due to thermoelectric current as driving force. This significantly can influence the estimations of the lifetime of the ITER tungsten divertor.

References

- [1] E.P. Vaulin et al., Sov. J. Plasma Phys. Vol.7, No 2 (1981) 239 - 242
- [2] S.Takamura et al., Phys.Plasmas, Vol.5, No 5 (1998) 2151-2158
- [3] V.Phillipps et al., Nucl.Fusion, Vol.33, No 6 (1993) 953-961